

Improved Fracture Toughness of Cryorolled and Room Temperature Rolled 6082 Al Alloys

Vineet Kumar · I. V. Singh · B. K. Mishra · R. Jayaganthan

Received: 4 September 2013/Revised: 1 November 2013/Published online: 24 April 2014
© The Chinese Society for Metals and Springer-Verlag Berlin Heidelberg 2014

Abstract In the present work, 6082 Al alloy has been rolled to 40% and 70% thickness reductions at the cryogenic and room temperatures for the improvement in mechanical and fracture toughness properties. All cryorolled samples are subjected to aging at different temperatures, i.e., 140, 160, and 190 °C to improve the strength, ductility, and fracture toughness. The microstructures of the cryorolled (CR) and room temperature rolled (RTR) alloy after 40% and 70% thickness reductions are characterized by FE-SEM to reveal the modes of failure. The results show that the starting bulk Al alloy specimen is fractured in total ductile manner, consisting of well-developed dimples over the entire surface. The mechanical properties and fracture toughness of the 70% CR alloy are found better than 70% RTR alloy due to higher dislocations density and formation of sub-grain structures in the CR alloy.

KEY WORDS: 6082 Al alloy; Rolling; Mechanical properties; Fracture toughness; *J*-Integral; Material characterization

1 Introduction

The development of the high strength Al alloys for aerospace and automobiles applications is growing day by day due to extending the service life of the components manufactured from these alloys [1, 2]. The mechanical properties of the 6082 Al alloy can be further improved by severe plastic deformation (SPD). SPD is an assured method to produce ultrafine-grain (UFG) materials with attractive properties. The techniques of SPD are rapidly growing, and are on the verge of moving from lab-scale

research to commercial products. Although, SPD techniques have already demonstrated their capability by significantly refining the microstructure, but they still need to be optimized for producing specific UFG structure along with desirable material properties [3, 4]. SPD describes a group of the metal working techniques which involves extreme plastic straining of the material to produce UFG structure by imposing very high shear deformations under hydrostatic pressure. SPD leads to exceptional grain refinement of the material without introducing any significant changes in the overall dimensions of the specimen or work piece [5]. Huges and Hansen [6] and Wei et al. [7] observed the formation of ultrafine grains in the cryorolled Al alloy due to high density of dislocations, and effective suppression of the dynamic recovery during cryorolling. The severe strain induced at very low temperature facilitates the formation of sub-structure, and subsequently ultrafine grains [8–10]. Nowotnik et al. [11] analyzed the parameters (time and aging temperature) of precipitation strengthening which may lead to the most favorable mechanical properties of 6082 alloys.

Available online at <http://link.springer.com/journal/40195>

V. Kumar · I. V. Singh (✉) · B. K. Mishra
Department of Mechanical and Industrial Engineering,
Indian Institute of Technology, Roorkee, India
e-mail: ivsingh@gmail.com

R. Jayaganthan
Department of Metallurgical and Materials Engineering,
Indian Institute of Technology, Roorkee, India

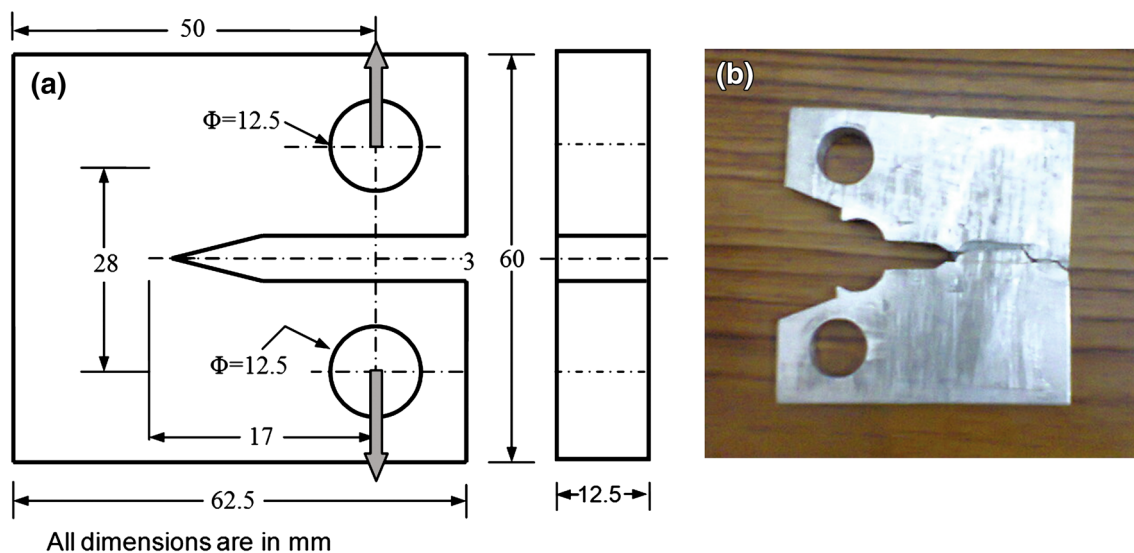


Fig. 1 a Dimensions of the CT specimen for fracture toughness test, b actual broken CT specimen

In the present work, the effects of cryorolling and room temperature rolling have been observed on the mechanical and elasto-plastic fracture toughness (J_{1c}) of 6082 Al alloy. The alloy is rolled at the cryogenic and room temperature for different thickness reductions. The compact tension (CT) tests are performed on bulk, cryorolled, and room temperature rolled specimens prepared as per ASTM E399-08 [12], E1820-11 [13], and E647-08 [14] standards. The results show that the microstructure, mechanical properties, and fracture toughness are strongly affected by severe plastic deformation process.

2 Experimental

The 6082 aluminum alloys have the following chemical composition: 1.20 wt% Si, 0.78 wt% Mg, 0.50 wt% Mn, 0.30 wt% Fe, 0.14 wt% Cr, 0.08 wt% Cu, 0.05 wt% Zn, and rest is Al. The material received from Virat Aluminum, Mumbai, India is cut into to small plates. These plates are then heat treated up to 540 °C, and maintained at this temperature approximately for two hrs followed by quenching in water at room temperature [15]. After this process, these plates are rolled at the cryogenic temperature so as to get the thickness reductions of 40% and 70%. After a single rolling pass, these plates are soaked in the liquid nitrogen for 15 min, and then again pass between the rollers until a desired thickness reduction is achieved. The rolling parameters are taken as: rolled diameter is 110 mm and rolling speed is 8 r/min. A solid lubricant MoSi₂ is used to reduce the frictional heat. The temperature before and after the rolling of the sample is found as -195 and -160 °C, respectively. The time between two successive

rolling passes is nearly found as 40–50 s. In a single pass, a thickness reduction of about 5% is achieved. Finally, to improve the mechanical and fracture properties, the cryorolled samples after 40% and 70% thickness reductions are subjected to aging at 140, 160, and 190 °C. The room temperature rolling is also carried out for 40% and 70% thickness reductions so as to characterize the microstructures and mechanical properties of the RTR samples.

After aging treatment, the tensile tests are performed in order to determine the strength and ductility of the CR and RTR Al alloy samples. The hardness is measured by applying a load on the specimen for 15 s on a plane parallel to the longitudinal axis (rolling direction) through Vickers hardness (HV) test. The surface of the specimen is polished mechanically using an emery paper and cleaned by a smooth cloth prior to each hardness measurement to ensure a bright surface. For every cleaned surface, on an average ten measurements are taken for hardness values.

The sub-size tensile specimens are prepared parallel to the rolling direction with a gauge length of 25 mm in accordance with ASTM E-8/E8 M-09 standard [16]. The tensile test is performed after polishing the samples in air at room temperature. The cryorolled samples after thickness reductions are machined before performing the tensile test.

The fracture toughness behavior of 6082 Al alloy is examined through the compact tension (CT) test. The CT specimens are prepared from bulk, CR, and RTR Al alloys after different thickness reductions. A typical CT specimen geometry along with the dimensions is shown in Fig. 1a, whereas Fig. 1b shows an actual broken CT specimen. All specimens are fatigue pre-cracked for a crack length/width ratio (a/w) of 0.5 following the ASTM standard E647-08 [14]. The pre-cracking is carried out on a computer-

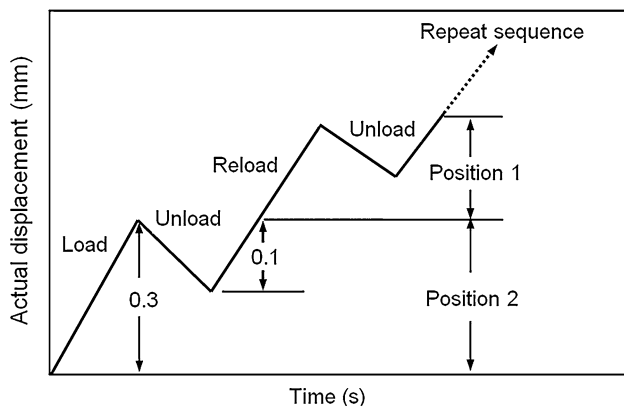


Fig. 2 Loading position of the fracture toughness test

controlled servo hydraulic Instron machine (model-1352). The pre-cracking is done at a stress ratio (R) of 0.1 at 10 Hz frequency. The pre-cracking before plane strain fracture toughness test is carried out as per the guidelines of ASTM standard E399-08 [12] and E1820-11 [13] on a 50 kN servo hydraulic Instron machine (model-1342). A displacement rate of 0.003 mm/s is applied at ambient temperature. The loading sequence applied for fracture test is shown in Fig. 2. A clip gauge with a travel of 5 mm is attached to separate the pieces of external knife-edge, near the machine notch at a spacing of 5 mm. For fracture toughness test, the load line displacement (LLD) plots are

shown in Fig. 3a–d for bulk, 40%-CR, 70%-CR, 40%-RTR, and 70%-RTR alloys, respectively. The LLD data for each of the specimen are recorded for subsequent analysis. The test is stopped when the maximum drop in load becomes more than 20%. This criterion is selected to maintain uniformity in all fracture toughness tests. After the completion of the fracture tests, all specimens are post-fatigue cracked, till separation to mark the stable crack growth region. In order to represent the fatigue pre-cracked regime, and stable crack growth regime under monotonic loading, the long samples of about 20 mm are cut from the central plane of the fractured surfaces.

The phenomena such as recovery, recrystallization, and precipitation hardening need to be controlled through the optimum aging condition for enhancing the strength and ductility simultaneously to a considerable extent. Hence, the CR 6082 Al alloy samples with 40% and 70% thickness reductions are subjected to aging treatment at 190, 160, and 140 °C for 14 h.

3 Results and Discussion

3.1 Effect of Heat Treatment

Figure 4a and b shows the variation of the hardness with aging time for different aging temperatures. From these figures, it is evident that the hardness first increases and

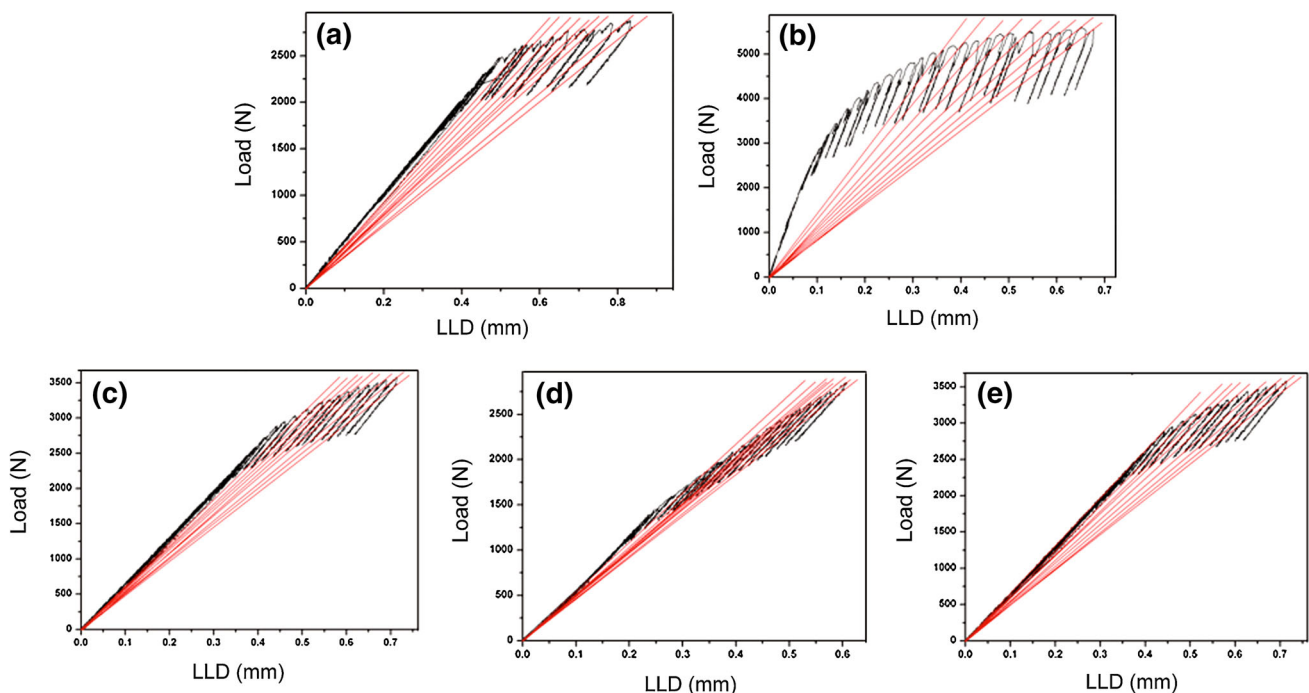


Fig. 3 Plot of load with load line displacement (LLD) for bulk alloy **a**, 40% CR alloy **b**, 70% CR alloy **c**, 40% RTR alloy **d**, 70% RTR alloy **e**

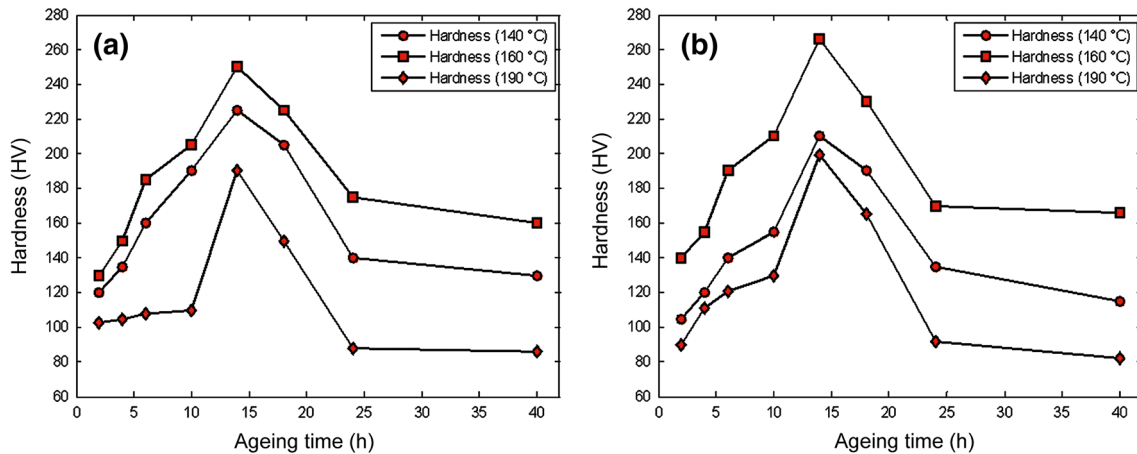


Fig. 4 Plots of Vicker's hardness versus. ageing time: **a** 40% CR alloy, **b** 70% CR alloy

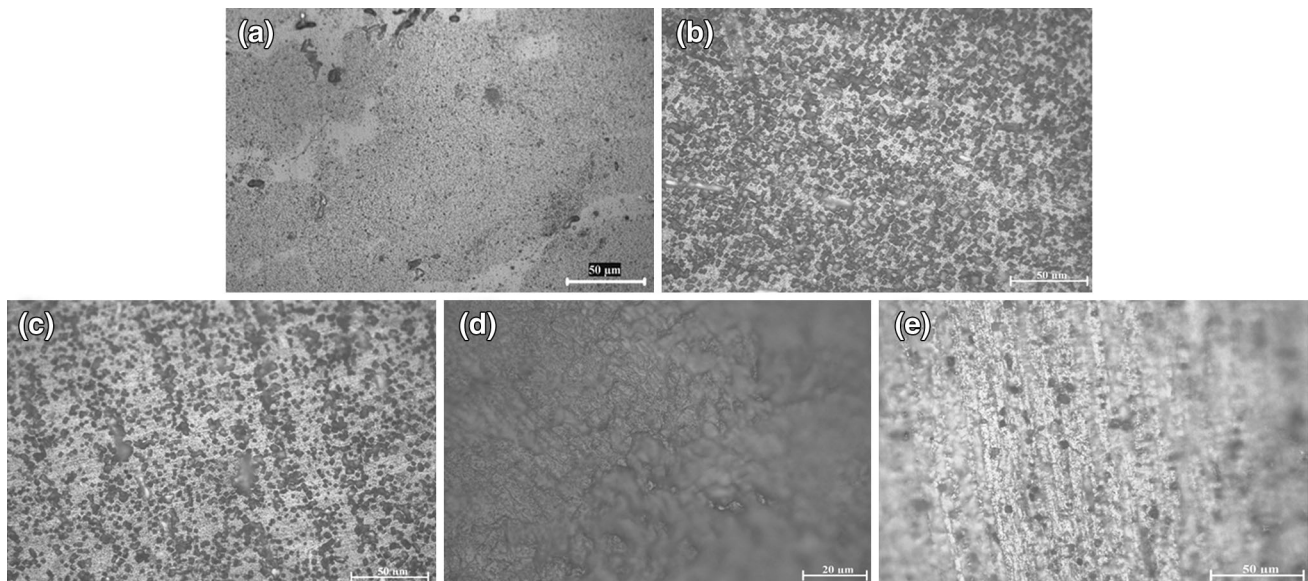


Fig. 5 Optical micrographs of bulk alloy **a**, 40% CR alloy **b**, 70% CR alloy **c**, 40% RTR alloy **d**, 70% RTR alloy **e**

then decreases with the aging time for the given aging temperatures, i.e., 190, 160, and 140 °C. This is due to the dynamic recovery of the grains in the CR samples. The effect of the sub-structure coarsening is prevalent as compared to precipitation hardening mechanism. In the case of age-treated specimens, the peak is found at 160 °C in the all the specimens corresponding to the aging time of 14 h for 40% and 70% thickness reductions.

3.2 Microstructure Characterization

Figure 5 depicts the optical micrograph of the bulk alloy, CR, and RTR 6082 Al alloy after 40% and 70% thickness reductions. The microstructures of the bulk alloy show the lamellar grains having average grain size of around 77 μm,

lying parallel to the ingot axis. In the case of CR samples, the average grain size is reduced to around 700 nm for 40% thickness reduction and 620 nm for 70% thickness reduction, whereas in the case of RTR samples, the grain size is reduced to around 900 nm for 40% thickness reduction and 760 nm for 70% thickness reduction.

The microstructural features of the bulk, 40%, 70% CR and RTR samples are shown in Fig. 6. It is evident that dislocation content increases with increasing deformation strain in the materials and it is higher for CR 70% as compared to RTR sample due to effective suppression of dynamic recovery. The grains are fragmenting effectively in the CR alloy and tend to form sub-grain structure due to the reassembly of dislocation density in the heavily deformed structures in the materials.

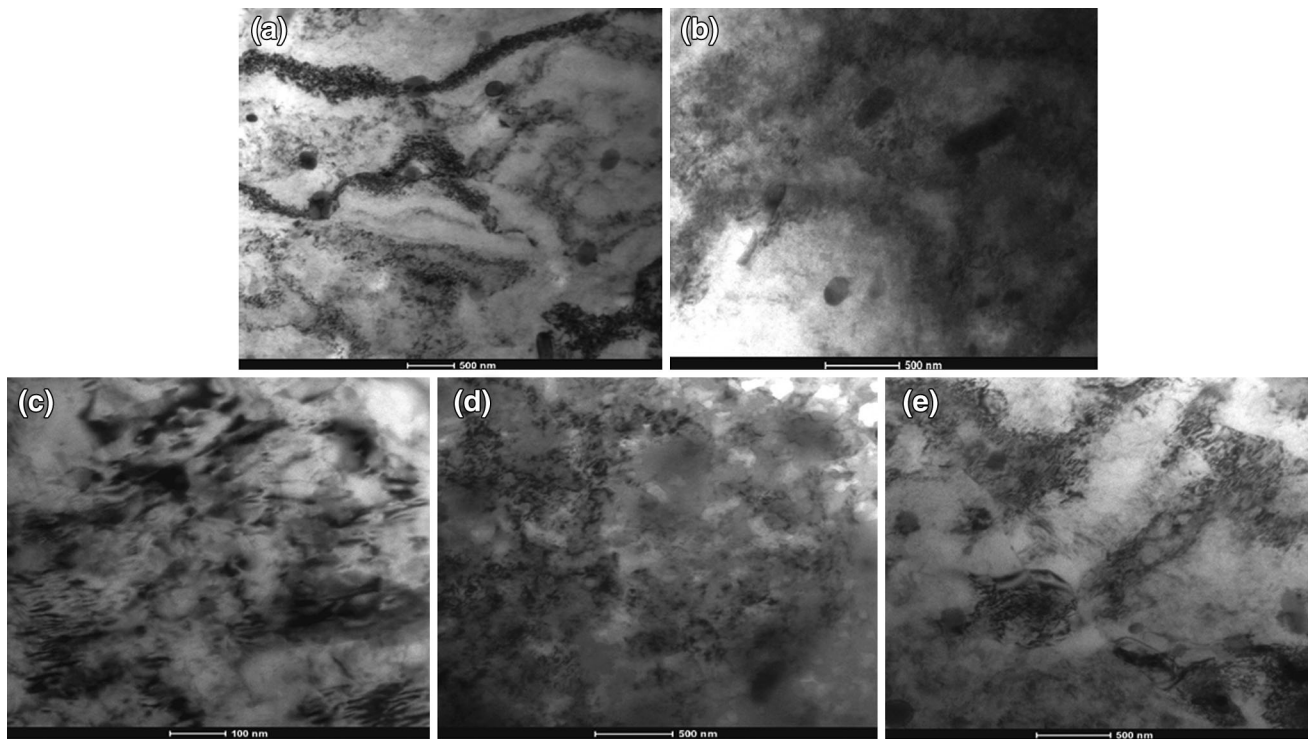


Fig. 6 TEM images of bulk alloy **a**, 40% CR alloy **b**, 70% CR alloy **c**, 40% RTR alloy **d**, 70% RTR alloy **e**

Table 1 Mechanical properties of the initial, CR, and RTR 6082 Al alloy

Sample	Yield strength, σ_y (MPa)	Tensile strength, σ_s (MPa)	Elongation (%)
40%-CR	370.0	350.6	13.5
40%-RTR	330.0	358.6	13.9
70%-CR	380.0	388.8	14.0
70%-RTR	350.0	380.8	11.2
Initial alloy	260.3	340.0	12.0

3.3 Mechanical Properties

Table 1 shows the effect of cryorolling over the tensile properties of the alloy. The modulus of elasticity (E) and Poisson’s ratio (ν) of the alloy is taken as 72 GPa and 0.33, respectively. In the case of cryorolling, a significant improvement in the mechanical properties of 6082 Al alloy is achieved as compared to starting bulk and RTR alloys, which may be due to the high amount dislocation density and ultrafine-grain formation [2, 17, 18].

3.4 Calculation of J_{1C}

From a compact tension specimen test, J is calculated as

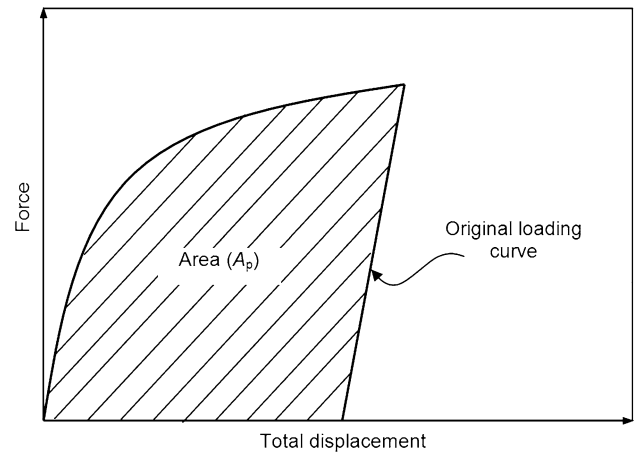


Fig. 7 Hatched area used for J -calculation

$$J = J_e + J_p, \tag{1}$$

where J_e is elastic component of J , and J_p is plastic component of J . For mode-I loading, J_{eI} and J_{pI} can be defined as

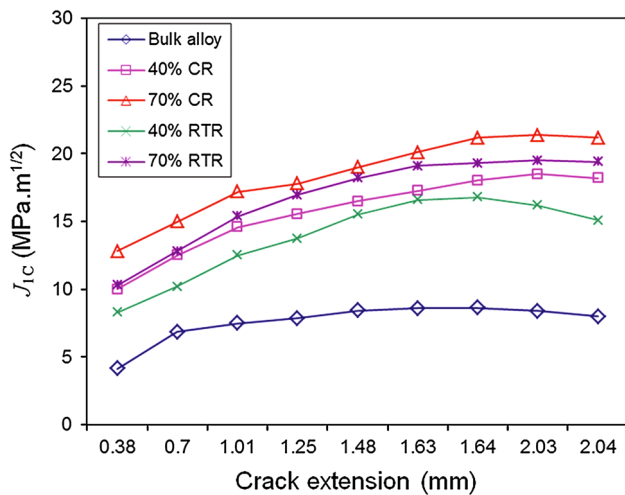
$$J_e = \frac{K^2(1 - \nu^2)}{E}, \tag{2}$$

$$J_p = \frac{\eta_p A_p}{B_N b_0}, \tag{3}$$

where

Table 2 Measured values of elastic–plastic fracture toughness (J_{IC})

Crack extension (mm)	Elastic–plastic fracture toughness (J_{IC}), MPa m ^{1/2}				
	Bulk alloy	CR		RTR	
		40%	70%	40%	70%
0.38	4.15	10.00	12.80	8.30	10.29
0.70	6.84	12.50	15.00	10.20	12.80
1.01	7.34	14.30	16.40	12.20	14.92
1.25	7.84	15.56	17.80	13.75	16.96
1.48	8.43	16.48	19.00	15.51	18.20
1.63	8.58	17.25	20.12	16.60	19.10
1.64	8.64	18.04	21.20	16.80	19.30
2.03	8.39	18.50	21.40	16.20	19.50
2.04	7.99	18.20	21.20	15.10	19.40

**Fig. 8** Fracture toughness of bulk, 40% CR, 70% CR, 40% RTR, and 70% RTR alloy

$$K = \frac{P}{(BB_N W)^{1/2}} f\left(\frac{a}{W}\right), \quad (4)$$

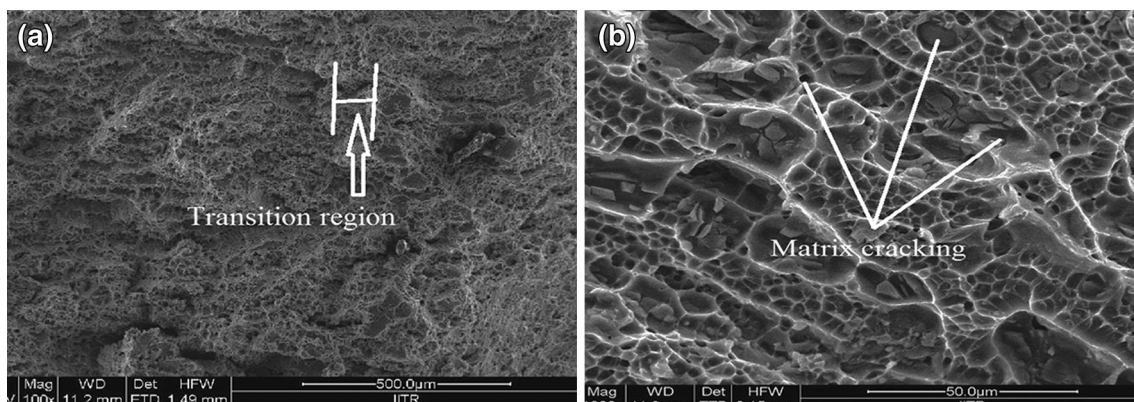
with $f\left(\frac{a}{W}\right) = \frac{(2+\frac{a}{W})\{0.886+4.64(\frac{a}{W})-13.32(\frac{a}{W})^2+14.72(\frac{a}{W})^3-5.6(\frac{a}{W})^4\}}{(1-\frac{a}{W})^{3/2}}$, where A_p is the area under force versus displacement as shown in Fig. 7; B_N is the net specimen thickness, $B_N = B$ if no side grooves are present; b_0 is un-cracked ligament, i.e., $(W - a_0)$; $\eta_p = 2 + 0.522 (b/W)$.

The fracture toughness test is carried out for bulk, CR, and RTR Al alloy samples. Elasto-plastic fracture toughness (J_{IC}) of the 6082 Al alloy is calculated using above relationship obtained from ASTM standard 1820-11. Table 2 shows the various values of elastic–plastic fracture toughness (J_{IC}) with crack extension. These values are also plotted in Fig. 8 with crack extension.

In the case of bulk Al alloy, the minimum fracture toughness (J_{IC}) is found to be 4.15 MPa m^{1/2} corresponding to a crack extension of 0.38 mm, whereas the maximum fracture toughness is found to be 8.64 MPa m^{1/2} corresponding to a crack extension of 1.64 mm.

In the case of 40%-CR aluminum alloy, the minimum J_{IC} is found to be 10.0 MPa m^{1/2} corresponding to a crack extension of 0.38 mm, whereas the maximum J_{IC} is found to be 18.50 MPa m^{1/2} corresponding to a crack extension of 2.03 mm. For 70% CR alloy, the minimum J_{IC} is found to be 12.80 MPa m^{1/2} corresponding to a crack extension of 0.38 mm and the maximum J_{IC} is found to be 21.40 MPa m^{1/2} corresponding to a crack extension of 2.03 mm.

In the case of 40%-RTR alloy, the minimum value of J_{IC} is found as 8.30 MPa m^{1/2} corresponding to a crack extension of 0.38 mm, whereas the maximum J_{IC} is found to be 16.80 MPa m^{1/2} corresponding to a crack extension of 1.64 mm. For 70%-RTR Al alloy, the minimum J_{IC} is found to be 10.29 MPa m^{1/2} corresponding to a crack extension of 0.38 mm, and the maximum J_{IC} is found to be

**Fig. 9** FE-SEM images of the fracture surface of the bulk alloy: **a** transition region (fatigue pre crack and fracture), **b** fracture surface (*enlarged view*)

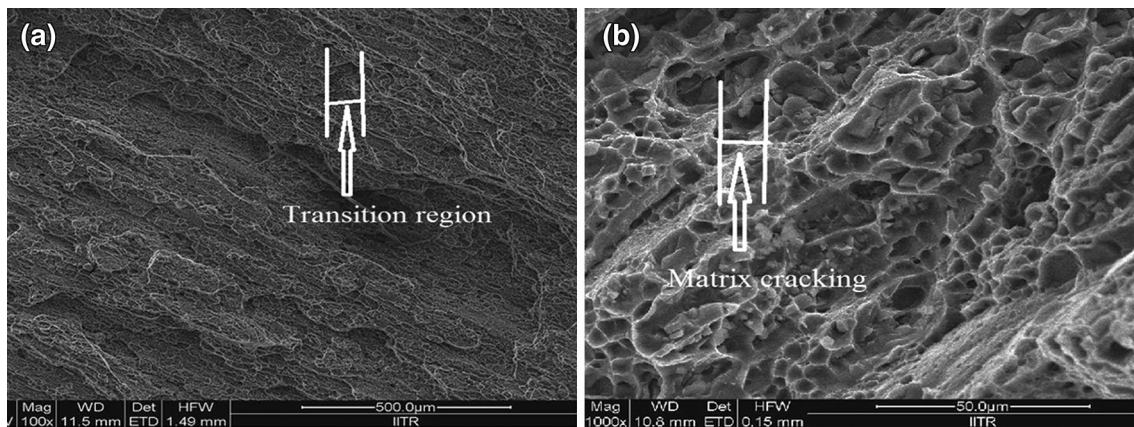


Fig. 10 FE-SEM images of the fracture surface of 40% CR alloy: **a** transition region (fatigue pre crack and fracture), **b** fracture surface (enlarged view)

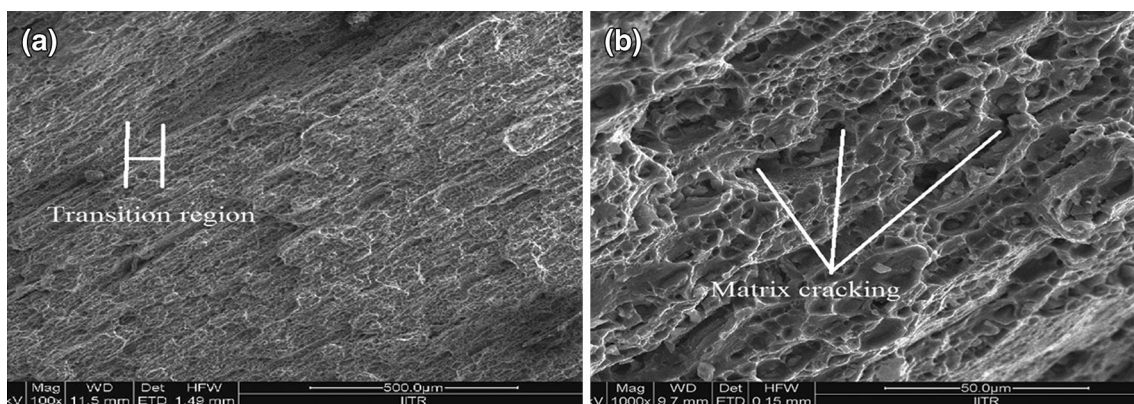


Fig. 11 FE-SEM images of the fracture surface of 70% CR alloy: **a** transition region (fatigue pre crack and fracture), **b** fracture surface (enlarged view)

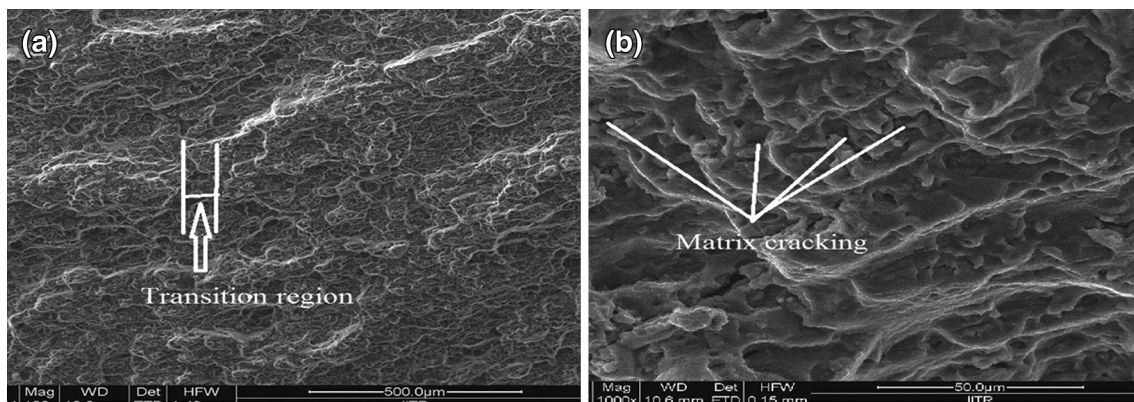


Fig. 12 FE-SEM images of the fracture surface of 40% RTR alloy: **a** transition region (fatigue pre crack and fracture), **b** fracture surface (enlarged view)

19.50 MPa m^{1/2} corresponding to a crack extension of 2.03 mm.

These results show that there is drastic improvement in fracture behavior of 6082 Al alloy after the cryorolling and

the room temperature rolling, which is mainly due to the increased fracture stress and grain-boundary strengthening. The maximum improvement in fracture toughness is found to be 155% for 70%-CR alloy and 132% for 70%-RTR

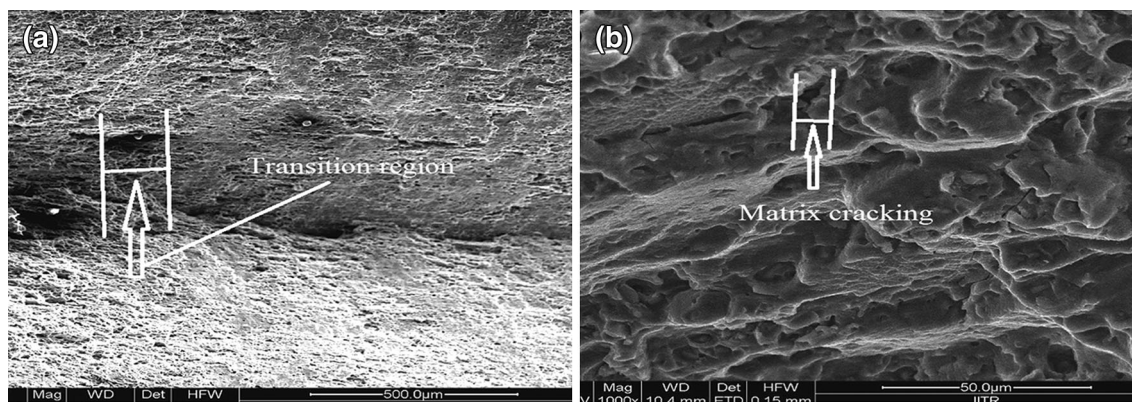


Fig. 13 FE-SEM images of the fracture surface of 70% RTR alloy: **a** transition region (fatigue pre crack and fracture), **b** fracture surface (enlarged view)

alloy. The improvement in fracture behavior is found to be more for CR alloy as compared to RTR alloy, which is mainly due to sub-structure and ultrafine-grain formation in the case of CR alloy.

3.5 Fracture Surface Morphology

Fracture micrographs (FE-SEM) of the various CT specimens are obtained, and are shown in Figs. 9, 10, 11, 12, and 13 for bulk, CR, and RTR Al alloy. Figure 9 shows the FE-SEM of the fractured surface for the bulk alloy, whereas Figs. 10 and 11 show the FE-SEM of 40%-CR and 70%-CR Al alloy, respectively. Figures 12 and 13 show the images of fractured surface of 40%-RTR and 70%-RTR alloys, respectively.

The rough fracture surfaces with large dimples show a ductile fracture implying a void-coalescence fracture mechanism for all the cases. The dimples are formed due to void growth and coalescences at different materials processing conditions. Transition region is clearly visible as shown in all the cases. Limited region of quasi-cleavage fracture can be noticed in these sites corresponding to local embrittlement or limited plastic deformation of the matrix in Figs. 10b and 11b. In addition, more regions of quasi-cleavage fracture are noticed with increase in aging time. Damage mechanism is transformed from the striation governed smooth fatigue failure during pre-cracking into void growth- and coalescence-driven ductile fracture under monotonic loading. It is known that the dimple size is dependent on the inclusion size. With the increase in precipitates due to aging, the number of second phase particles increase in matrix, which increases the resistance to the dislocation movement [19–21]. The average dimple size of the starting bulk alloy is found to be 77 μm , which decreases with the increase in thickness reduction obtained by the cryorolling as shown in Fig. 10 for 40%-CR alloy

and in Fig. 11 for 70%-CR alloy. The dimple size gets reduced to less than 1 μm after 70% thickness reduction. This is the reason why the grain refinement and work hardening occurs during the rolling process. Similar, reasons are reported in literature for severely deformed samples.

The FE-SEM observations of the RTR 40% and RTR 70% are also performed, which show also that the RTR alloy also fail in ductile manner consisting of many dimples over the entire surface as shown in Figs. 12 and 13. These results show that the elongated dimples on the surface are the result of the void nucleation and coalescence by the strong shear deformation and fracture process on the shear plane as shown in Figs. 12b and 13b.

The present study show that there is significant improvement in the mechanical and fracture properties of 70%-CR sample as compared to initial and RTR samples, which may be due to the formation of higher dislocation density and sub-grain structures in the CR samples as compared to RTR [2, 17, 18].

4 Conclusions

In this work, tensile and fracture behaviors of bulk, CR, and RTR 6082 Al alloy are investigated through mechanical and fracture tests. The fracture toughness testing of the bulk and deformed alloy is carried out using ASTM E-1820-11 and E-399-09 standards. The elasto-plastic fracture toughness, J_{1C} was obtained for initial, 40%-CR, 70%-CR, 40%-RTR, and 70%-RTR alloy samples. On the basis of the present study, the following conclusions can be drawn:

- (1) The rolled alloy shows a substantial plasticity along with sub-critical crack growth as can be seen from the load displacement plots, which may be due to the involvement of secondary cracks from the precipitates.

- (2) A drastic improvement in the fracture toughness (J_{1c}) was observed for CR and RTR Al alloy as compared to the bulk material which is due to the increased fracture stress and grain-boundary strengthening.
- (3) The improvement in fracture toughness is found to be more for CR Al alloy as compared to RTR Al alloy.
- (4) FE-SEM fractographs of the samples revealed that the starting bulk Al alloy specimen was fractured in a total ductile manner, consisting of well-developed dimples over the entire surface along with big size precipitates.
- (5) A substantial increase in the yield strength and fracture toughness of CR and RTR Al alloy is found, which may be due to the high density of dislocations, sub-grain structure formations, and high volume fraction of grain boundaries in the deformed alloy.

References

- [1] S.K. Panigrahi, R. Jayaganthan, Mater. Sci. Forum **584–586**, 734 (2008)
- [2] S.K. Panigrahi, R. Jayaganthan, Mater. Sci. Eng. A **480**, 299 (2008)
- [3] Z. Vaiev, Adv. Eng. Mater. **5**, 296 (2003)
- [4] C.L. Terry, R.Z. Valiev, JOM **56**, 64 (2004)
- [5] A. Nikolaos, S. Antonis, C. John, Mech. Mater. **58**, 55 (2013)
- [6] D. Huges, N. Hansen, Acta Mater. **45**, 3871 (1997)
- [7] Q. Wei, S. Cheng, K. Ramesha, E. Ma, Mater. Sci. Eng. **381**, 71 (2004)
- [8] N. Rajasekaran, V. Sampath, J. Min. Mater. Charact. Eng. **10**, 527 (2011)
- [9] P. Das, S. Dutta, H. Roy, R. Jayaganthan, Int. J. Technol. Eng. Syst. **2**, 143 (2011)
- [10] R. Valiev, R. Islamgaliev, I. Alexandrov, Prog. Mater Sci. **45**, 103 (2000)
- [11] G. Nowotnik, J. Sieniawski, A. Nowotnik, J. Achiev. Mater. Manuf. Eng. **17**, 105 (2006)
- [12] E647-08, Standard Test Method for Measurement of Fatigue Crack Growth Rates, Annual Book of ASTM Standards (2008)
- [13] E1820-11, Standard Test Method for Measurement of Fracture Toughness, Annual Book of ASTM Standards (2008)
- [14] E399-08, Standard Test Method for Linear-elastic Plane-strain Fractures Toughness K_{Ic} of Metallic Materials, Annual Book of ASTM Standards (2008)
- [15] X. Gomez, L. Galdos, C. Garcia, J. Eng. Mater. Technol. **131**, 501 (2009)
- [16] E8/E8 M-09, Standard Test Methods for Tension Testing of Metallic Materials, Annual Book of ASTM Standards (2009)
- [17] S.K. Panigrahi, R. Jayaganthan, Mater. Sci. Eng. A **528**, 3147 (2011)
- [18] D. Singh, P.N. Rao, R. Jayaganthan, Mater. Des. **50**, 646 (2013)
- [19] H. Somekawa, T. Mukai, Scr. Mater. **53**, 1059 (2005)
- [20] S. Chang, S. Seo, S. Lee, C. Kang, S. Hong, S. Dong, Mater. Sci. Forum **449**, 589 (2004)
- [21] G. Nowotnik, Archiv. Mater. Sci. Eng. **29**, 93 (2008)